

LITERATURE CITED

- Wall, M. C., and K. J. Laidler, "The Molecular Kinetics of the Urea-Urease System. IV. The Reaction in an Inert Buffer," *Arch. Biochem. Biophys.*, **43**, 312 (1953).
- Ramachandran, K. B., and D. D. Perlmutter, "Effects of Immobilization on the Kinetics of Enzyme-Catalyzed Reactions. II. Urease in a Packed-Column Differential Reactor System," *Biotechnol. Bioeng.*, **18**, 685 (1976).

- Heineken, F. G., H. M. Tsuchiya, and R. Aris, "On the Mathematical Status of the Pseudo-Steady State Hypothesis of Biochemical Kinetics," *Mathematical Bioscience*, **1**, 95 (1967).
- Aris, R., "Mobility, Permeability, and the Pseudo-Steady-State Hypothesis," *ibid.*, **13**, 1 (1972).

Manuscript received July 23, 1976; revision received September 15 and accepted Sept. 16, 1976.

Hydrogenolysis Kinetics of Ethane and *n*-Pentane Over Unsupported Copper/Nickel and Platinum Catalysts

Two kinetic models of hydrocarbon hydrogenolysis over monometallic surfaces, based respectively on catalytically uniform or nonuniform surfaces, are applied to ethane and *n*-pentane hydrogenolysis results over copper-nickel alloy catalysts as well as the monometallic catalysts platinum and nickel. If no direct hydrogen desorption appears in any postulated irreversible step, both models predict the same composition for the important surface intermediates C_nH_x ($n = 1, s$), where x depends upon the catalyst.

This analysis predicts that for essentially all alloy catalysts to which the postulated sequences may apply, the hydrogenolytic surface intermediate C_nH_x contains one more hydrogen atom than that calculated for a nickel catalyst: specifically, C_2H_3 (alloy) vs. C_2H_2 (nickel) for ethane and C_5H_6 (alloy) vs. C_5H_7 (nickel) for *n*-pentane.

DAVID F. OLLIS
and
HASSAN TAHERI

Department of Chemical Engineering
Princeton University
Princeton, New Jersey 08540 USA

SCOPE

The hydrogenolysis of ethane is by now a classical reaction in heterogeneous catalysis, having been characterized kinetically by studies over iron, cobalt and nickel catalysts (Cimino et al., 1954), other group VIII metals (Sinfelt and Taylor, 1968), and copper-nickel alloys (Sinfelt et al., 1972; Sinfelt, 1973). An obvious industrial interest has existed for some time in finding base metal alloy catalysts which might be used as a substitute for such noble metals as platinum and palladium. In the petroleum refining industry, reactions of C_5 , C_6 , and C_7 hydrocarbons are important; in particular, the selectivity for hydrogenolysis vs. nondestructive rearrangements [(de)hydrocyclization, skeletal isomerization, dehydrogenation] is of prime concern.

It has been appreciated previously that copper-nickel catalysts, in the presence or absence of solid acid catalysts, exhibit lower hydrogenolytic activity than nickel toward both ethane (Sinfelt et al., 1972) and C_5 - C_7 hydrocarbons (Reman et al., 1971; Ponoc and Sachtlar, 1972). A kinetic scheme involving equilibrated hydrocarbon adsorption on a catalytically uniform surface has been proposed by Cimino et al. (1954) and subsequently modified by Sinfelt (1972) to rationalize reaction orders in ethane and hydrogen at temperatures where hydrogenolysis rates

first become appreciable. An alternate proposal set forth by Boudart (1972) considers this reaction as a two-step irreversible sequence occurring on a catalytically non-uniform surface for several monometallic nickel or iron catalysts.

The purpose of the present paper is to establish that either scheme provides a reasonable description of hydrogenolysis reaction orders over copper-nickel alloy surfaces, in particular, for the alkanes, ethane (Sinfelt et al., 1972), and *n*-pentane (Taheri, 1975; Taheri and Ollis 1975). Further, the results provide a quantitative connection between hydrogenolysis kinetics of alkanes over copper-nickel alloys vs. the well-studied examples of monometallic nickel or platinum catalysts.

The implications of these results are twofold. First, the utility of ethane hydrogenolysis models in developing fruitful approaches to hydrogenolysis of ethane and considerably larger molecules over metal alloy catalysts encourages application of other classical kinetic laws to reactions catalyzed on alloy surfaces. Also important, the present paper provides a quantitative experimental example of the nearly identical kinetic features resulting from considering catalytic surfaces as either uniform or nonuniform.

CONCLUSIONS AND SIGNIFICANCE

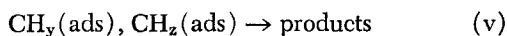
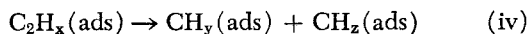
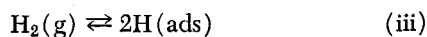
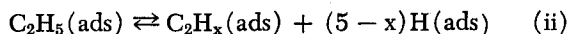
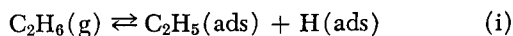
The hydrogenolysis of ethane and of *n*-pentane over bulk, granular copper-nickel alloys, nickel, and platinum appears susceptible to analysis with either the classical scheme first developed for ethane hydrogenolysis over pure group VIII metals as modified by Sinfelt (1972) or by treatment as a two-step irreversible sequence (Boudart, 1972). The result does not increase our understanding of the uniformity vs. nonuniformity of the hydrogenolysis sites, but either view produces the same picture for the composition of the major adsorbed intermediate C_nH_x

($n = 2, 5$). Thus, changes in the composition of this intermediate with alloy composition do provide insights into hydrogenolytic selectivity of the alloy surfaces examined.

The present study also finds hydrogenolysis kinetics for *n*-pentane to be the same over platinum and most copper-nickel alloys examined with respect to hydrogen and *n*-pentane reaction orders. This result quantifies the often loosely stated argument that copper/nickel alloys may be catalytically more similar to platinum than to nickel.

REACTION SEQUENCE

According to Sinfelt (1972), the hydrogenolysis of ethane over nickel and platinum metals may be represented by the following scheme:



where (iv) is the presumed slow step, ethane and hydrogen adsorption are taken to be equilibrated, and step (ii) is also presumed to be at equilibrium. As Sinfelt (1973) has discussed, the assumption of ethane adsorption equilibrium appears valid, provided the temperature is not too high. By the now classical arguments, the hydrocarbon coverage is assumed to be unaltered by the presence of surface hydrogen, and the rate of the presumed slow step is taken proportional to the coverage of the assumed predominant species C_2H_x :

$$\text{rate} = k\theta_{C_2H_x} \quad (1)$$

If this coverage is taken to be Langmuirian (uniform surface)

$$\theta_{C_2H_x} = \frac{K P_{C_2H_6} / P_{H_2}^{(3-x/2)}}{1.0 + K P_{C_2H_6} / P_{H_2}^{(3-x/2)}}$$

then over a relatively small variation of pressures a simple approximation results in a power law expression

$$\theta_{C_2H_x} = [K' P_{C_2H_6} / P_{H_2}^{(3-x/2)}]^n \quad (2)$$

where $0 < n < 1.0$ and $K' \neq K$. The predicted rate form (1) becomes (3)

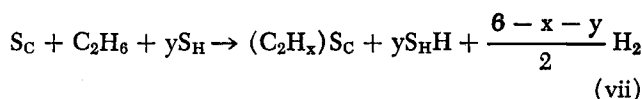
$$\text{rate}(\text{predicted}) = k(K')^n P_{C_2H_6}^n P_{H_2}^{-(3-x/2)n} \quad (3)$$

By comparison of experimentally observed orders n' and m' for C_2H_6 and H_2 , respectively, as determined from Equation (4)

$$\text{rate}(\text{observed}) = k' P_{C_2H_6}^{n'} P_{H_2}^{m'} \quad (4)$$

evidently $n = n'$ and $x = [6 - 2(m'/n')]$.

The alternative interpretation for ethane hydrogenolysis kinetics suggested by Boudart (1972) is given by Equations (vi) to (viii):



where S_H , S_C are surface sites for hydrogen and hydrocarbon, respectively.

The important differences between this treatment and the earlier sequence (i) through (v) are the following.

Adsorption of ethane is treated as an irreversible step.

The surface is assumed to be nonuniform in two senses: two different adsorption sites S_C and S_H for ethane and hydrogen, respectively, are assumed, and the hydrocarbon sites S_C are taken to be kinetically nonuniform.

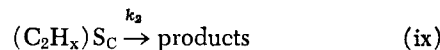
The resulting equation proposed for ethane hydrogenolysis in a two-step irreversible sequence was shown to be

$$\text{rate} = k P_{C_2H_6}^{(1-M)} P_{H_2}^{M - \frac{y}{2}(1-M)} \quad (5)$$

where M is a constant.

It appears implausible that hydrogen released as H_2 in step (vii) should return in the same form as a reactant in step (viii). A simpler model would assume that no molecular hydrogen participates in the second slow step. The first slow step (vii) partitions the hydrogen removed from the hydrocarbon into two forms: that adsorbed as (HS_H) and gaseous H_2 . As will be shown from analysis of ethane and *n*-pentane data, it may not be necessary to invoke such partitioning.

We therefore consider a modified interpretation such that step (vii) above is left intact, and step (viii) is modified to give



The equation for the irreversible sequence (vi) + (vii) + (ix) is obtained from Equation (21) of Boudart (1972) [the rate equation from which (5) is derived] but now uses a hydrogen pressure exponent of 0 for the second irreversible step. The result is Equation (6):

$$\text{rate} = k P_{C_2H_6}^{(1-M)} P_{H_2}^{M - \frac{y}{2}(1-M)} \quad (6)$$

The parameter M reflects surface nonuniformity (Appendix), and it is calculated from the equation $(1-M) = n'$ (ethane pressure exponent). The number of hydrogen adsorption sites y is available from use of both experimental pressure exponents, in particular, $y = 2m'/$

TABLE 1. SUMMARY OF KINETIC PARAMETERS FOR ETHANE HYDROGENOLYSIS ON COPPER NICKEL ALLOYS AND PLATINUM
(FROM SINFELT ET AL., 1972; SINFELT, 1973)

Composition (at % copper)	Temperature range (°C)	E^a	r_0^b	n^c	Reaction orders m^d	Temp. (°C) ^e
0	226-268	43	2.1×10^{31}	1.0	-2.1	238
6.2	308-339	51	3.2×10^{31}	0.9	-1.3	331
10.3	326-356	51	1.1×10^{31}	—	—	—
31.5	355-396	50	6.0×10^{29}	—	-1.3	377
42.4	352-395	51	5.2×10^{29}	0.9	-1.3	384
52.7	383-408	50	2.0×10^{29}	0.8	-1.2	399
63.3	383-440	48	1.8×10^{28}	0.8	-1.2	420
74.0	424-455	47	6.5×10^{27}	—	—	—
(Pt)	344-385	54	5.9×10^{31}	0.9	-2.5	(357)

- a. Apparent activation energy, kcal/mole.
b. Preexponential factor, moles/s-cm²
c. Order with respect to ethane.
d. Order with respect to hydrogen.
e. Temperature at which the reaction orders were determined.

$(1 - M) = 2m'/n'$. The value of x which reveals the composition of the hydrocarbon fragment C_2H_x is not determined from this interpretation. Note, however, from Equation (vii) that the value of y allows calculation of the maximum possible value of x , namely, $y + x_{\max} = \text{total hydrogens in ethane} = 6$. Thus, $x_{\max} = 6 - y = 6 - 2(m'/n')$, which is exactly the equation for calculation of x in the uniform surface model.

RESULTS AND DISCUSSION

Ethane Hydrogenolysis on Unsupported Copper/Nickel and Platinum

The ethane hydrogenolysis data of Sinfelt et al. (1972) are summarized in Table 1. The data appear to fall neatly into two groups: the pure nickel surface (for which $E = 43$ kcal/mole and the hydrogen pressure exponent is -2.1) and all bimetallic catalyst surfaces (for which the activation energy measured $E = 47$ to 51 kcal/mole and the hydrogen pressure exponent is -1.2 to -1.3). This categorization suggests that the predominant surface intermediate $C_2H_x(\text{ads})$ is the same on all alloy surfaces but differs from that predominant on a pure nickel surface.

Insertion of the reported values for m' and n' (Table 1) results in the calculated x values of Table 2 (uniform surface column). These latter numbers suggest that on pure nickel the major dehydrogenated species $C_2H_x(\text{ads})$ in step (iv) above is $C_2H_2(\text{ads})$, whereas on the alloy surfaces the final species is apparently $C_2H_3(\text{ads})$. From the method of calculation, it is not surprising that the result yields an intermediate which has the same stoichiometric formula for all bimetallic surfaces yet is different from that for nickel. The same calculation for the platinum results also listed in Table 1 leads to $x = 0.45$ (or 0, taking the nearest integral value). Thus it appears that hydrogenolysis catalysts such as bimetallic copper/nickel or platinum which are less active for this reaction than nickel may have predominant hydrogenolysis precursor species which are either more or less hydrogenated than

that predicted for nickel, each of the former cases leading to a higher activation energy presumably reflecting step (iv) above.

It is also evident from the reaction orders for ethane in Table 1 that n' is higher on nickel than for platinum or any bimetallic catalyst, suggesting a relatively weaker adsorption of the species C_2H_x on nickel.

For the nonuniform surface model, the results of calculating y (and x_{\max}) are shown in Table 2, columns 6 and 7. Two features are noteworthy:

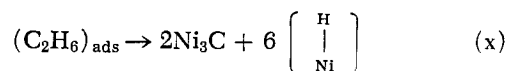
The value for y in this nonuniform surface model is essentially constant over all alloy surfaces but different from that for pure nickel.

The value of M is zero or close to zero (the interpretation of this result depends upon the equilibrium adsorption isotherm of the hydrocarbon reactant, see Appendix).

The value of x_{\max} is, of course, identical to x in every case, since the same equation is used in the calculation (x or x_{\max}) $= 6 - 2(m'/n')$.

The constant value of y over all (but one) alloy surfaces suggests that on the latter catalysts, the total size of the major hydrogenolysis site ($S_c + yS_H$) is smaller by one hydrogen site than that for pure nickel.

The postulated sequence (vii) allows two fates for hydrogen removed from the adsorbed species: direct desorption or transfer to surface sites S_H followed by equilibration with gas phase hydrogen through step (vi). Martin and Imelik (1974) report that ethane adsorbed at low coverages on nickel and heated to 200° to 300°C produced a magnetic bond number of 12 consistent with the structure below:

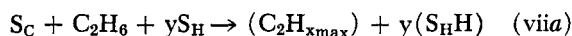


Thus, no direct hydrogen desorption from the surface intermediate was implicated. As the hydrogenolysis orders in ethane are at or near unity, Table 1, we may expect

TABLE 2. KINETIC MODEL PARAMETERS FOR ETHANE HYDROGENOLYSIS

Alloy catalyst bulk % copper	Experimental data		(Uniform surface) x	Nonuniform surface		
	n (ethane order)	m (hydrogen order)		y	x_{\max}	m
0	1.0	-2.1	1.8(2)	4.2	1.8(2)	0
6.2	0.9	-1.3	3.1(3)	2.9	3.1(3)	0.1
31.5	0.9	-1.3	3.1(3)	2.9	3.1(3)	0.1
42.4	0.9	-1.3	3.1(3)	2.9	3.1(3)	0.1
52.7	0.8	-1.2	3.0(3)	3.0	3.0(3)	0.2
63.3	0.8	-1.2	3.0(3)	3.0	3.0(3)	0.2
(Pt)	0.9	-2.5	0.45(0-1)	5.55	0.45(0-1)	0.1

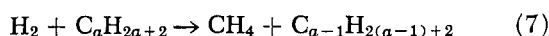
the hydrocarbon coverage under hydrogenolysis conditions to be low; hence it seems reasonable to assume that x_{\max} represents the composition of the adsorbed intermediate ($C_2H_{x_{\max}}$) deduced from the interpretation of nonuniform surface kinetics. The final form of equation (vii) is reasonably taken to be (vii') on all metal and alloy surfaces in the following discussion [this step may be relatively simple, since (S_C and yS_H) may be a single surface entity]:



Thus, in this simplest interpretation, both kinetic models predict the same composition for the major intermediate in ethane hydrogenolysis.

***n*-Pentane Hydrogenolysis on Unsupported Copper/Nickel and Platinum**

Literature reports indicate that *n*-paraffin hydrogenolysis over nickel surfaces usually involves the cleavage of a terminal carbon-carbon bond, the initial hydrogenolytic event being typified by Equation (7) (Kochloeff and Bazant, 1968; Kikuchi and Morita, 1969; Matsumoto et al., 1970):

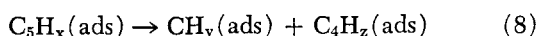


For bimetallic copper-nickel catalysts prepared in substantially the same manner as those of Sinfelt et al. (1972), we find a similar result for *n*-pentane hydrogenolysis (Taheri, 1975): for low conversions of *n*-pentane, the major products are again methane and *n*-butane. (At higher conversions, achieved in our studies with higher temperatures, *n*-pentane isomerization is also important.) Thus, we are led to attempt to represent the initial hydrogenolysis kinetics of *n*-pentane over such nickel and bimetallic catalysts (and platinum) by the same conceptual scheme as above for ethane.

The determinations of reaction orders m' and n' for hydrogen and *n*-pentane, respectively, are presented in Table 3. As typically observed earlier for ethane, the dependence of rate on reactant pressures is positive with hydrocarbon (*n*-pentane) and negative for hydrogen. Perhaps more striking, the values of m' and n' from Table 3 are seen to remain approximately constant over all bimetallic catalysts exhibiting a negative hydrogen pressure dependency, for example, from about 90 to 50 atomic % nickel in Table 3. (Positive H_2 orders and 0 order in *n*-pentane indicate a coking catalyst).

Several differences are also evident. For *n*-pentane, the reaction order in hydrogenolysis is higher on alloys than on nickel, the converse behavior being observed for ethane on similar alloys. The hydrogen pressure exponents also change in the sense opposed to that for ethane in bimetallic catalysts, however, the value of this exponent is nearly the same on the copper/nickel catalysts for either reaction.

The large negative partial pressure influences of hydrogen on the rate of *n*-pentane hydrogenolysis suggest that a kinetic sequence similar to those previously discussed for ethane may be present. If the equivalent representation of steps (i) to (v) is assumed for *n*-pentane, then the slow step should now be written as



The same arguments which have been used frequently for ethane now predict that the *n*-pentane hydrogenolysis rate should vary according to

$$\text{rate} = k (K')^n P_{C_5}^n P_{H_2}^{n(6-x/2)} \quad (9)$$

TABLE 3. KINETIC MODEL PARAMETERS FOR *n*-PENTANE HYDROGENOLYSIS

Copper	Experimental data		Uniform surface x	Nonuniform surface		
	% (pentane order)	(hydrogen order)		m	y	x_{\max}
0	0.30	-1.05	5.0(5)	0.7	7.0	5.0(5)
7.8	0.45	-1.35	6.0(6)	0.55	6.0	6.0(6)
16.7	0.50	-1.50	6.0(6)	0.50	6.0	6.0(6)
26.4	0.45	-1.60	4.9(5)	0.55	7.1	4.9(5)
38.5	0.47	-1.40	6.3(6)	0.53	6.0	6.0(6)
50.3	0.44	-1.34	5.9(6)	0.56	6.1	5.9(6)
(Pt)	0.41	-1.25	5.9(6)	0.59	6.1	5.9(6)

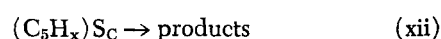
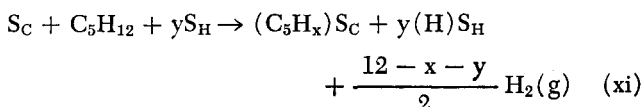
where x again represents the number of hydrogens remaining on the C_5 entity involved in the left-hand side of the slow step [Equation (8)]. The exact and nearest integral values of x so calculated from the *n*-pentane and hydrogen pressure exponents are given in the fourth column of Table 3. The main features are seen to be that

1. All of the bimetallic catalysts (73.6% nickel excepted) exhibit a value for x essentially equal to 6 vs. 5 found for nickel, suggesting a less dehydrogenated major species on the alloy surfaces.

2. As with ethane, the predicted difference in hydrogen content of the species undergoing the slow step in the presumed sequence is only a single hydrogen between nickel vs. the results for the copper-nickel alloys.

3. Platinum, a catalyst with weaker *n*-pentane hydrogenolysis tendencies than nickel, behaves analogously to all of the alloys (73.6% nickel again excepted) for which negative reaction orders were determinable. (The positive hydrogen orders for 35.2 and 27.3% nickel indicate the deposition of carbon due to the higher temperatures utilized, Table 3.)

The analogy of Equations (vi), (vii), and (ix) are (vi) (unchanged), (xi), and (xii):



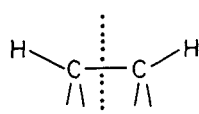
Calculation of M , y , and x_{\max} for *n*-pentane as before for ethane leads to the last three columns of Table 3. These results indicate that the value of M is much larger for C_5 hydrogenolysis than for ethane. Again, since the model assumptions are unchanged from those for ethane, x_{\max} is identical to x for the uniform surface model *n*-pentane. In contrast to the result for ethane, the *n*-pentane value of (x , x_{\max}) for platinum is identical to the predominant value on copper-nickel surfaces.

In the following discussion, x_{\max} is taken to represent the composition of $(C_5H_x)_{ads}$ as was earlier argued to be correct for ethane.

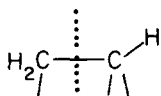
For either ethane or *n*-pentane, the value of x calculated for C_nH_x ($n = 1, 5$) in the presumed rate determining step is found to be a constant on all alloy surfaces (73.6% nickel excepted for $n = C_5$) for which negative hydrogen pressure exponents were observed, that is, all surfaces to which the postulated sequences might reasonably apply. With both reactants, the nearest integral value of x is usually larger by one on the alloy surfaces than on nickel. Thus, the kinetic analysis above provides the suggestion that ethane and *n*-pentane hydrogenolysis proceed through similar kinetic sequences on pure nickel or copper-nickel alloy surfaces.

The remaining discussion appears most conveniently presented around the following three points:

ETHANE

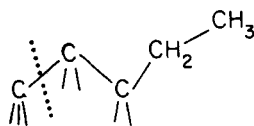


(Ni, $x=2$)

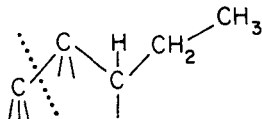


(Ni/Cu, $x=3$)

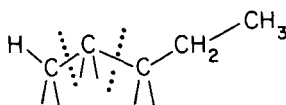
n-PENTANE



(Ni, $x=5$)



or



(Ni/Cu, Pt, $x=6$)

Fig. 1. Possible structures for surface intermediates of composition C_2H_x or C_5H_x , where x takes the values shown in Tables 2 and 3. The carbon to surface bonds indicate only the supposed number of bonds formed; no postulate is made as to exactly how many catalyst surface atoms participate. The additional H atom for the species C_5H_6 is postulated to occur on the terminal carbon at the lowest temperatures studied (Table 3) but on either terminal or central carbon at slightly higher temperatures (see text).

1. The nature of the copper/nickel surfaces of our study compared to those of Sinfelt et al. (1972) for ethane hydrogenolysis.

2. The elimination of other possible reactions for n -pentane which could alter the proposed sequence above.

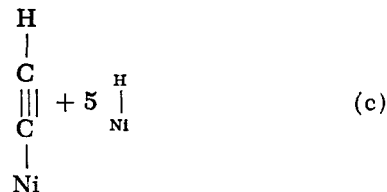
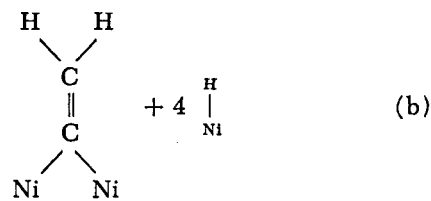
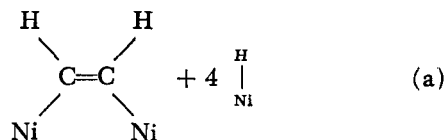
3. The proposal of a reasonable structure for the species C_5H_x or C_2H_x in the irreversible steps.

Taking up these points in order, our catalysts were prepared in substantially the same manner as those used by Sinfelt et al. (1972), ending with a final 16 hr reduction at 350°C in hydrogen. With the aid of pulsed H_2 chemisorption technique analogous to that pioneered for carbon monoxide by Gruber (1962) and applied to platinum by Freel (1972), we show elsewhere (1975, 1976) that the relative amount of H_2 chemisorbed at room temperature falls from 1.0 on nickel to an approximately constant value of 0.1 for alloys of bulk compositions in the range 25 to 75% copper. This result is in good agreement with the fraction of strongly adsorbed hydrogen reported by Sinfelt et al. (1972) and with H_2 chemisorption for copper-nickel films reported by van der Plank and Sachtler (1972) and Ponc and Sachtler (1972), the latter group reporting a value of $14 \pm 7\%$ of the pure nickel value for alloys in the same intermediate composition range as above. Thus, static (Sinfelt et al., 1972) or pulse (present) H_2 chemisorption on similarly prepared granular catalysts provide the same results and agree nicely with relative H_2 chemisorption fractions on evaporated alloy films (sintered at 200°C).

Hydrocarbons larger than ethane clearly may undergo a variety of possible reactions. At low conversions reported here, the only other important reactions of n -pentane is isomerization to isopentane, neopentane or cyclopentane not being noted. We report elsewhere (Taheri, 1975; Taheri and Ollis, 1976) that both hydrogenolysis and isomerization rates pass through a maximum value as the hydrogen pressure is decreased, indicating the onset of carbon deposition typically accompanied by a shift from negative to positive hydrogen exponents. As these maxima are observed at a different hydrogen pressure for each reaction, it is reasonable to suppose that the two reactions of isomerization and hydrogenolysis occur on different parts of the alloy surfaces, thus allowing our consideration of only one important species $C_5H_x(ads)$ in the discussion above for hydrogenolysis kinetics at low conversions.

There remains the proposal of plausible surface structures for the intermediates C_2H_x and C_5H_x predicted from Table 2 and 3 for ethane and n -pentane hydrogenolysis, respectively. A nonunique set of such adsorbed intermediates is presented in Figure 1. For each intermediate, it is reasonable to suppose that there remains but a single carbon-carbon bond to be cleaved to achieve hydrogenolysis. The ethane species $C_2H_2(ads)$ and $C_2H_3(ads)$ for nickel and copper/nickel respectively, taken with the presumed participation of two (or more) surface metal sites in S_c leads easily to the plausible structures shown for C_2H_x ($x=2, 3$) in Figure 1.

The result $x = x_{max} = 2$ and $y = 4$ for ethane on pure nickel is in agreement with recent models of Dalmon, Candy, and Martin (1976) deduced from saturation magnetization changes following ethane chemisorption at near ambient temperatures. Their method of measurement yields an average magnetic bond number which they interpret as the number of single bonds formed with nickel atoms per molecule adsorbed. As this number equals six for ethane (prior to hydrogenolysis) on nickel, these authors offer three adsorbed structures consistent with this value:



Each model above is also observed consistent with magnetic bond number values of 4 and 2 for ethylene and acetylene adsorption, respectively. The first two structures offer two examples where $x=2$ for $(C_2H_x)_{ads}$. As these represent average values, we cannot say whether these are the major adsorbed C_2 species or whether a wide range of x values for C_2H_x exists on nickel. Ethane adsorption on copper-nickel alloys at 20°C yields lower

bond numbers than found for nickel (Martin and Imelik 1974), consistent with the general picture from Table 2 that the C_2 intermediates on copper-nickel surfaces are less dehydrogenated than those on pure nickel.

The proposed carbon-carbon double bond of the adsorption intermediates of Dalmon et al. (1976) may be viewed as alternate possibilities to the single bond structures of Figure 1. The intermediate in the French study of adsorption at ambient temperatures is claimed by these authors to be degraded into a completely hydrogen free pair of isolated carbon atoms at $T \cong 70^\circ\text{C}$. Thus, the achievement of carbon-carbon single bond structure at the higher hydrogenolysis temperatures of the ethane and *n*-pentane studies in the presence of hydrogen seems more reasonable to propose (Figure 1) than the concerted one-step hydrogenolysis of a carbon-carbon double bond.

A logical structure for $C_5H_x(\text{ads})$ is less obvious. If the values in Table 3 are taken at face value, then 6 or 7 of the original hydrogens have been removed from the adsorbed *n*-pentane prior to hydrogenolysis. Assignment again of single C—C bonds to the dehydrogenated carbons leads plausibly but not uniquely to the two structures proposed. These structures might give the behavior observed below in the present study (Taheri, 1975):

1. Initial hydrogenolysis of *n*-pentane leads largely to production of methane and *n*-butane; thus the species $C_5H_x(\text{ads})$ must be adsorbed beginning at one end of the fragment. Assignment of the highest multiple bonding to the terminal carbon would likely lead to a predominant production of methane.

2. The triadsorbed species (alpha, beta, and gamma carbons bonded to surface) allows easy visualization of further terminal degradation of *n*-butane to *n*-propane, etc., which is observed on nickel (and to a much lesser extent on high percent nickel alloys catalysts) at higher temperature or higher conversions (Taheri, 1975).

3. Over the alloys, especially those lower in nickel content, and over platinum we observe that slightly higher temperatures lead to the formation of considerable and equal amounts of ethane and propane. Assignment of the additional H atom predicted for the alloy and platinum surface hydrogenolysis intermediate to the gamma carbon at the lowest temperatures and to the alpha carbon or gamma carbon at higher temperatures might rationalize the lessening rate of subsequent demethylations at the former temperatures and the appearance of larger but essentially equal amounts of ethane and propane at higher temperatures for the alloy catalysts and for platinum.

While it is tempting to relate the proposed structures of $C_5H_x(\text{ads})$ to easier skeletal isomerization, which is observed on copper/nickel and platinum catalysts vs. nickel, this appears to be incorrect for the alloys for two reasons. First, the isomerization reaction seems to occur on a different part of the alloy surface as mentioned earlier. Second, an analysis of the orders of the isomerization reaction with respect to hydrogen and hydrocarbon leads to the proposal of a more hydrogenated adsorbate in the presumed isomerization sequence (Taheri, 1975; Taheri and Ollis, 1976).

ACKNOWLEDGMENT

The authors are pleased to thank the National Science Foundation and the American Chemical Society for continued support during this study.

LITERATURE CITED

Boudart, M., *Kinetics of Chemical Processes*, pp. 189-193, Prentice Hall, Englewood Cliffs, N.J. (1968).

———, "Two-Step Catalytic Reaction," *AIChE J.*, **18**, 465 (1972).

Cimino, A., M. Boudart, and H. S. Taylor, "Ethane Hydrogenation-Cracking on Iron Catalysts With or Without Alkali," *J. Phys. Chem.*, **58**, 796 (1954).

Dalmon, J. A., J. P. Candy, and G. A. Martin, "Magnetic Study of Ethane and Benzene Adsorption on Cu/Ni/SiO₂: Correlation with the Catalytic Activity," Private communication (1976).

Freel, J., "Chemisorption on Supported Platinum I. Evaluation of a Pulse Method," *J. Catalysis*, **25**, 139 (1972).

Gruber, H. L., "An Adsorption Flow Method for Specific Metal Surface Area Determination," *Anal. Chem.*, **34**, 1828 (1962).

Kikuchi, E., and Y. Morita, "Hydrogenolysis of *n*-Pentane on Nickel Catalyst," *J. Catalysis*, **15**, 217 (1969).

Kochloeff, K., and V. Bazant, "Hydrogenolysis of Saturated Hydrocarbons on a Nickel Catalyst," *ibid.*, **10**, 140 (1968).

Martin, G. A., and B. Imelik, "Adsorption of Hydrocarbons and Various Gases on Ni-SiO₂ Catalysts Studied by High Field Magnetic Methods," *Surface Science*, **42**, 157 (1974).

Matsumoto, H., Y. Sato, and Y. Yoneda, "Contrast Between Nickel and Platinum Catalysts in Hydrogenolysis of Saturated Hydrocarbons," *J. Catalysis*, **19**, 101 (1970).

Ponec, V., and W. M. H. Sachtler, "The Reactions Between Cyclopentane and Deuterium on Nickel and Nickel-Copper Alloys," *ibid.*, **24**, 250 (1972).

Reman, W. G., A. H. Ali, and G. C. A. Schuit, "Alloy Formation on Zeolite Y," *ibid.*, **20**, 374 (1971).

Sinfelt, J. C., and W. F. Taylor, "Catalytic Hydrogenolysis of Ethane," *Trans. Faraday Soc.*, **64**, 3086 (1968).

Sinfelt, J. C., J. L. Carter, and D. J. C. Yates, "Catalytic Hydrogenolysis and Dehydrogenation over Copper-Nickel Alloys," *J. Catalysis*, **24**, 283 (1972).

Sinfelt, J. C., "Kinetics of Ethane Hydrogenolysis," *ibid.*, **27**, 468 (1972).

———, "Specificity in Catalytic Hydrogenolysis by Metals," *Adv. Catalysis*, **23**, 91 (1973).

Taheri, Hassan, "Characterization and Catalytic Activity of Copper-Nickel Alloys," Ph.D. thesis, Chemical Engineering, Princeton Univ., N.J. (1975).

———, and D. F. Ollis, paper presented at NYC-New England Catalysis Society Symposium, Yale Univ., New Haven, Conn. (1975).

———, submitted to *J. Catalysis* (1976).

Van der Plank, P., and W. M. H. Sachtler, "Surface Composition of Equilibrated Copper-Nickel Alloy Films," *J. Catalysis*, **24**, 250 (1972).

APPENDIX

In the derivation of a rate equation on nonuniform surfaces (see also Temkin, 1957, 1965; Boudart, 1968), the forward rate constants for Equations (vii) and (ix) are taken to have the forms

$$k_{vii} = k_{vii}^0 e^{-\alpha S}$$

and

$$k_{ix} = k_{ix}^0 e^{(1-\alpha)S}$$

where α = constant (transfer coefficient, $0 < \alpha < 1$), and S is a parameter giving a linear variation in the heat of adsorption for step (vii) in the forward direction:

$$\Delta H_{\text{ads}} = \Delta H_{\text{ads}}^0 - S/RT$$

The possible isotherms of step (vii) adsorption include those of Freundlich and Temkin:

$$\theta = \text{constant} \cdot P^\gamma \quad (\text{Freundlich})$$

$$\theta = \text{constant} \cdot \ln P \quad (\text{Temkin})$$

The meaning of M is given by

$$M = \alpha - \gamma \quad (\text{Freundlich})$$

$$M = \alpha \quad (\text{Temkin})$$

For ethane, M is always near 0 on nickel and the alloys (Table 2, column 7) thus $\alpha \sim \gamma$ (Freundlich) or $\alpha \sim 0$ (Temkin). In the latter case, the forward rate constant for

the first irreversible step is independent of S ; that is, this irreversible step on a nonuniform surface is indistinguishable from an irreversible step on a uniform surface.

Manuscript received April 20, 1976; revision received August 11, and accepted August 20, 1976.

Periodic Cycling of Plate Columns: Discrete Residence Time Distribution

The discrete residence time distribution applies to systems under periodic control. A system consisting of a plate column has been modeled to allow the generation of the discrete residence time distribution. The parameters in the model have been evaluated by measurements of entrainment, holdup, and the step response of the column under direct computer control. A least-squares minimization technique provided confirmation of the modeling procedures.

I. A. FURZER

and

G. J. DUFFY

University of Sydney
N.S.W. 2006, Australia

SCOPE

Periodic cycling is a technique that can be applied to all separation processes taking place in plate columns. The vapor flow to the column is switched on and off in a regular cycle, and liquid drains from plate to plate during the brief time the vapor flow is zero. The theory of this unsteady state processing has been developed for a linear equilibrium relationship and predicts a major increase in separating ability. These increases have been observed in small distillation columns, but in experimental studies on large columns and in gas absorption columns reported in the literature, the increases predicted by the theory could not be obtained. The reason for this difference has been reported as due to mixing

of the liquid as it drains from plate to plate when the vapor flow is zero. Conventional mixing models from plug flow to a series of well-mixed stages have been used to account for the mixing. However, there is little physical significance in using a model consisting of well-mixed stages. An improvement in modeling of the liquid mixing during the draining period is proposed in this paper, which has real physical significance. It consists of liquid being transferred from a plate to the next two successive plates below. A fraction of the liquid is retained and mixed on each of these two plates. This improvement in the understanding of the draining phenomenon can lead to the minimization of the liquid mixing and a closer approach between theory and experiment.

CONCLUSIONS AND SIGNIFICANCE

We have proposed a new liquid mixing model for the liquid draining period for plate columns under periodic control. This (2S) model allows liquid to penetrate to the two neighboring plates below. The model allows for the prediction of the holdup distribution on the plates, and the response to an impulse is the discrete residence time distribution, which is a characteristic of systems under periodic control. The two parameters in the (2S) model were evaluated from the step response of a column controlled from a PDP11/45 computer

We can conclude that a significant fraction of the liquid holdup on a plate bypasses the plate immediately

below and is retained by the second plate below. In our investigations we found 63% of the holdup was transferred to the plate below and 12.5% to the second plate below.

This liquid bypassing of a plate during the liquid draining period has a significant effect on the separating ability of the column. It considerably reduces the separation that is predicted by the normal theory of periodic cycling. The inclusion of the (2S) mixing model into the mass transfer theory of periodic control results in a more complex treatment and will appear later.

Danckwerts (1953) introduced the residence time distribution for continuous systems and uses the C distribution for the impulse response and the F distribution for the step response. The distributions allow for the identification of plug flow and perfectly mixed regions in a system. Departures from these extreme flow conditions can be accommodated by dead water, bypass streams and the use of

Correspondence concerning this paper should be addressed to I. A. Furzer.

the Peclet number to characterize longitudinal mixing. The Laplace transform of the C distribution or the impulse response is the transfer function of the system. If the output of the system is observed at fixed time intervals only, we can generate the Z transform of the system. Both of these transfer functions apply only to systems which have the properties of a continuous variable.

If the system is under periodic control, then the output is discontinuous and the use of continuous system variables